Vietnam Journal of Earth Sciences, 1-15, https://doi.org/10.15625/2615-9783/16442

Vietnam Academy of Science and Technology
Vietnam Journal of Earth Sciences
http://www.vjs.ac.vn/index.php/jse

A numerical investigation of the impact of shield machine's operation parameters on the settlements above twin stacked tunnels - A case study of Ho Chi Minh urban railway Line 1

Ngoc Anh Do[1]*, Trong Thang Dang[2], Daniel Dias[3,4]

[1]*Hanoi University of Mining and Geology, Faculty of Civil Engineering, Department of Underground and Mining Construction, Hanoi, Vietnam*
[2]*Vietnam Institute for Building Science and Technology - IBST, Hanoi, Vietnam*
[3]*Grenoble Alpes University, Laboratory 3SR, Grenoble, France*
[4]*Antea Group, Antony, France*

Received 13 May 2021; Received in revised form 29 July 2021; Accepted 13 August 2021

ABSTRACT

Three-dimensional finite difference calculations are proposed to investigate the influence of operation parameters of the shield machines during twin stacked tunnel excavation on the surface settlements. The numerical model is validated by experimental data obtained from Hochiminh's metro line 1 project, used as a reference case in this study. The parametric study focuses on the influence of the face support pressure, the grouting pressure, and the shield's length. The numerical results indicated that an increase in the face pressure and grouting pressure is not always followed by a decrease in surface settlements. A shorter shield machine causes smaller surface settlements to develop over single lower and twin stacked tunnels.

Keywords: twin stacked tunnels, numerical simulation, shield operation, face pressure, grouting pressure, shield length.

1. Introduction

The excavation of tunnels in the urban area usually causes a certain surface settlement which influences the stability structures and must be therefore well predicted. When using a shield machine, besides soil properties and support structures, the operation parameters of the shield machine play also an important role (Kasper and Meschke, 2006a; Kasper and Meschke, 2006b; Chakeri et al., 2013; Chakeri et al., 2014; Kim et al., 2018).

Kasper and Meschke (2006a, 2006b) proposed a three-dimensional finite element model for shield tunneling to analyse the influence of different soil parameters. The stiffness increases with the tail void grout, the cover depth, the face and grouting pressures on the surface settlements. A shield-driven tunnel advance in a homogeneous soft

*Corresponding author, Email: nado1977bb@gmail.com

cohesive soil below the groundwater table was considered. Accordingly, an increase in the face and/or grouting pressure is followed by a decrease in the surface settlement. Chakeri et al. (2013) presented the effect of tunnel diameter, surface surcharge, and face support pressure on the maximum surface settlement. The results of empirical and numerical methods were compared with observed data. Kim et al. (2018) introduced a numerical analysis that allows estimating the critical face pressure and backfill grouting pressure during the excavation of a shield tunnel. Unlike the results presented by Kasper and Meschke (2006b) and Chakeri et al. (2013), Kim et al. (2018) indicated that an increase of the face pressure and/or grouting pressure does not always follow by a decrease in the settlement. It should be noted that the above researches considered the case of a single tunnel.

When the tunnels are excavated at a closed distance to each other, it is important to predict the twin tunnels' interaction (Do et al., 2014a, 2014b). Interactions between closely spaced tunnels were studied in the literature using several approaches: physical model testing (Kim et al., 1998; Chapman et al., 2007; Ng. et al., 2013; Lu et al., 2019; Lu et al., 2019; Tran and Hiroshi, 2020), field observations (Suwansawat and Einstein, 2007; Chen et al., 2011; Ocak, 2013), empirical/analytical methods (Wang et al., 2003; Suwansawat and Einstein, 2007; Yang and Wang, 2011; Wang et al., 2018, Zhang et al., 2018; Zhang et al., 2020) and numerical modeling (Ercelebi et al., 2011; Hasanpour et al., 2012; Mirhabibi and Soroush, 2013; Do et al., 2014a; Chakeri and Unver, 2014; Chakeri et al., 2014, Janin et al., 2015; Sahoo and Kumar, 2018; Zhao et al., 2019; Shivaei et al., 2020; Ly et al., 2021). Most studies in the literature focused on the effect of the tunnel distance, relative position of tunnels, tunnel depth, and soil properties on the stability of tunnel lining, surrounding ground, and adjacent structures. However, the influence of the shield's operation parameters during twin tunnels excavation was rarely considered. Do et al. (2014b) introduced an interesting study on the effect of twin stacked tunnel excavation procedure on tunnel behavior. It was recommended that the lower tunnel should be excavated first and then followed by the upper tunnel to minimize the surface settlement and unfavorable interactions between stacked tunnels.

Metro systems are now under development in large cities in Vietnam as Hanoi capital and Ho Chi Minh city to follow the infrastructure expansion demands. Most of them are designed to include two parallel tunnels excavated at close distances from each other (Ho Chi Minh, 2016; MRB, 2012; Kuriki, 2020). In this study, a full 3D numerical model of twin stacked tunnels is used to evaluate the effect of the operation parameters of a shield machine on the surface settlement. Most of the main elements of a mechanized excavation are simulated in this numerical model: face pressure, conicity of the shield, grouting pressure, progressive hardening of the grout, jacking force, and lining joint pattern. Among them, special attention is paid to the effect of the following main parameters, including face pressure, grouting pressure at the shield tail, length, and therefore weight of the shield. Parameters of the Hochiminh's metro line 1 project in Vietnam are adopted in this study as a reference case.

2. Study case of the Hochiminh's subway project - metro line 1

Metro line 1 of Hochiminh's metro system consists of 14 stations and 19.7 km length, including 2.6 km underground and 17.1 km elevated section. One EPB-TBM is used to excavate twin tunnels of 6.82 m external diameter. Twin bored tunnels commence from KM 0+805 (end of Opera House station) to KM 1+586 (start of Ba Son station). The total length of each tunnel is approximately 780 m. The existing ground level is relatively flat. Twin tunnel bores at similar elevations were

commenced from Ba Son Station and transited to a stacked profile before ending at Opera House station. The maximum and minimum overburden is about 25 m and 12 m, respectively (Ho Chi Minh, 2016; Nguyen et al., 2020). The tunnels are excavated under a dense surface building area. In the middle of this underground route, the twin stacked tunnels closely underpass a building at chainage 0+980. Construction conditions of twin stacked tunnels at chainage 0+980 have been adopted as a reference case in this study. A schematic view of the transverse section where the twin tunnels are located near the surface building is presented in Fig. 1.

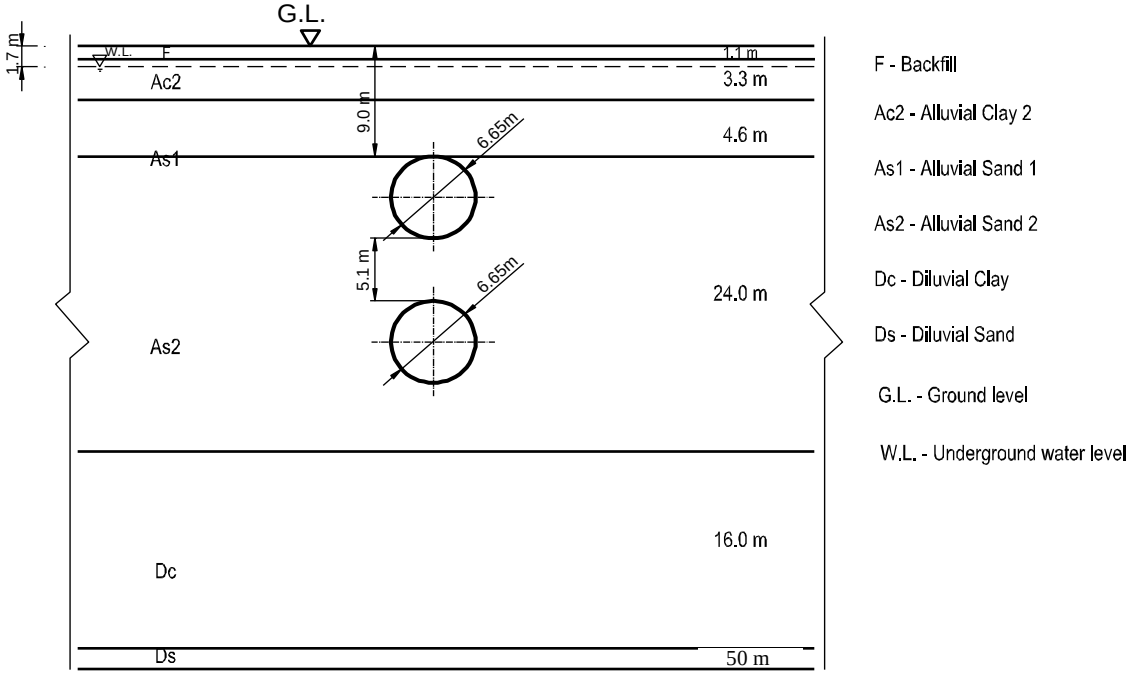

Figure 1. Geological conditions of the considered section (not scaled)

A mechanized tunneling method employing EPB-TBM has been used for excavating the twin tunnels. One EPB-TBM, which is equipped with a cutter-head of 6.82m in diameter and the shield machine's outer diameter of 6.79 m, bored the lower tunnel first. After finishing the first lower tunnel, the EPB-TBM was disassembled and then reassembled at the Opera House station to start excavating the second upper tunnel. Both tunnels are supported by six 30 cm thick concrete segment lining equal width (1.2 m). The external diameter of the lining of tunnels is 6.65m. The main parameters of TBM-EPB and segmental lining are presented in Table 1.

Table 1. Parameters of TBM-EPB machine and segmental lining (Ho Chi Minh, 2016)

Parameters	Value
Shield machine	
Excavation diameter (mm)	6820
Front shield diameter (mm)	6790
Tail shield diameter (mm)	6790
Segmental Lining	
Outer diameter (mm)	6650
Inner diameter (mm)	6050
Width (mm)	1200
Thickness (mm)	300
Number of segments	6
Young's modulus of concrete lining (MPa)	30,000

At chainage 0+980, the Hai Yen building was built after 1975 with six floors. The height is 5 m for the first floor and 3.5 m for the above floors. The building is made of reinforced concrete frames and brick walls. The building lies on shallow presumable woodpiles. The total length of the building axis along the tunnel route is 22 m, the width in the perpendicular direction is 18 m, and the height is 23 m. The main characteristics of the Hai Yen building are respectively provided in Table 2, Fig. 2.

Table 2. Main characteristics of Hai Yen building (Ho Chi Minh, 2016)

Feature	Value
Number of stories	6
Length of building (m)	22
Width of building (m)	18
Height of stories (m)	5(3.5)
Slab concrete thickness (cm)	12
Wall brick thickness (cm)	20
Young's modulus of concrete (MPa)	20,000
Wall brick elastic modulus (MPa)	2,000

a) Front view of the building Hai Yen

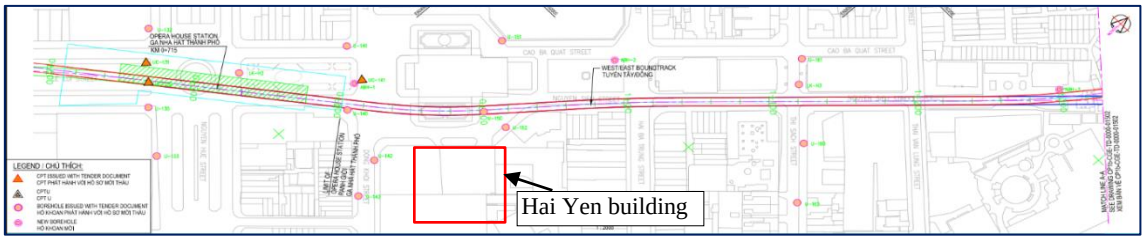

b) Plan view

Figure 2. Research site of the Hochiminh's metro line 1 (Ho Chi Minh, 2016)

Geotechnical conditions

The research site is characterized by the coastal plain topography, preliminary composed of saturated clay and sandy soils. The ground conditions in the area under study were investigated by in situ borehole measurement conducted by the contractor at the design stage. A total of six different strata were found: (1) fill layer, (2) Alluvial clay Ac2, (3) Alluvial sand As1, (4) Alluvial sand As2, (5) Diluvial clay Dc, and (6) Diluvial sand Ds. The tunnels cross mainly Alluvium sand layers, and most of the tunnel alignment is located under the groundwater table. The groundwater at investigated section is approximately 1.7 m below the ground level. Table 3 summarizes the primary geotechnical parameters of each soil layer. The soil effective strength parameters (c, ϕ) were determined from consolidated undrained triaxial compression tests. Pressure meter tests were used for the evaluation of the modulus of deformation.

Table 3. Geomechanical properties (Ho Chi Minh, 2016)

Properties/Soil layers	Backfill	Alluvial Clay (Ac2)	Alluvial Sand (As1)	Alluvial Sand (As2)	Diluvial Clay (Dc)	Diluvial Sand (Ds)
Thickness (m)	1.1	3.3	4.6	24.0	16	5
Unit weight γ (kN/m^3)	19	16.5	20.5	20.5	21.0	20.5
Mohr-Coulomb model						
ϕ (friction angle) (degrees)	25	24	30	33	22	35
c (cohesion) (kPa)	10	10	0	0	100	0
Poisson's ratio ν	0.37	0.48	0.33	0.31	0.45	0.3
ψ (dilation angle) (degrees)	0	0	0	0	0	0
Young's modulus E (MPa)	10	3	12.5	37.5	140	170
Plasticity Hardening model						
E_{50} (MPa)	10	3	12.5	37.5	140	170
E_{ur} (MPa	30	9	37.5	112.5	420	540
E_{oed} (MPa)	10	3	12.5	37.5	140	170
m	0.5	0.7	0.5	0.5	0.8	0.6
R_f	0.9					
P_{ref} (kPa)	100					
Normal consolidation coefficient K_0	1 - sinϕ					

3. Numerical simulation

Numerical simulation is conducted in this study using the Finite Difference Program FLAC^{3D} (Itasca, 2017). The tunnel construction is numerically modeled using a step-by-step approach (Melis et al., 2002; Ocak, 2013; Do et al., 2014a). The advance length of 1.2 m corresponds to an excavation cycle and equals the lining ring width installed at the shield tail. A schematic view of the present model is provided in Fig. 3.

In the 3D numerical model, most components of mechanized tunneling using shield machine are simulated: trapezoidal pressure applied on the tunnel face, circumferential pressure applied to the soil just behind the tunnel face, shield, and its conicity, self-weight of the shield machine, jacking forces applied on the lining ring at the shield tail, grouting pressure behind the shield tail and hardened grout, segmental lining with the joints and weight of the back-up train.

A trapezoidal profile of face pressure of EPB tunneling was applied from the shield chamber to the excavation face to account for the slurry density. The face pressures of 180

kPa and 310 kPa at the upper and lower tunnels centers, respectively, were chosen according to the field measurements at the Hochiminh subway project - metro line 1. Assuming the existence of a slight overcutting, a possible slurry migration could occur over right behind the cutting wheel. Therefore, pressure caused by the slurry solution has been applied to the cylindrical surface just behind the tunnel face.

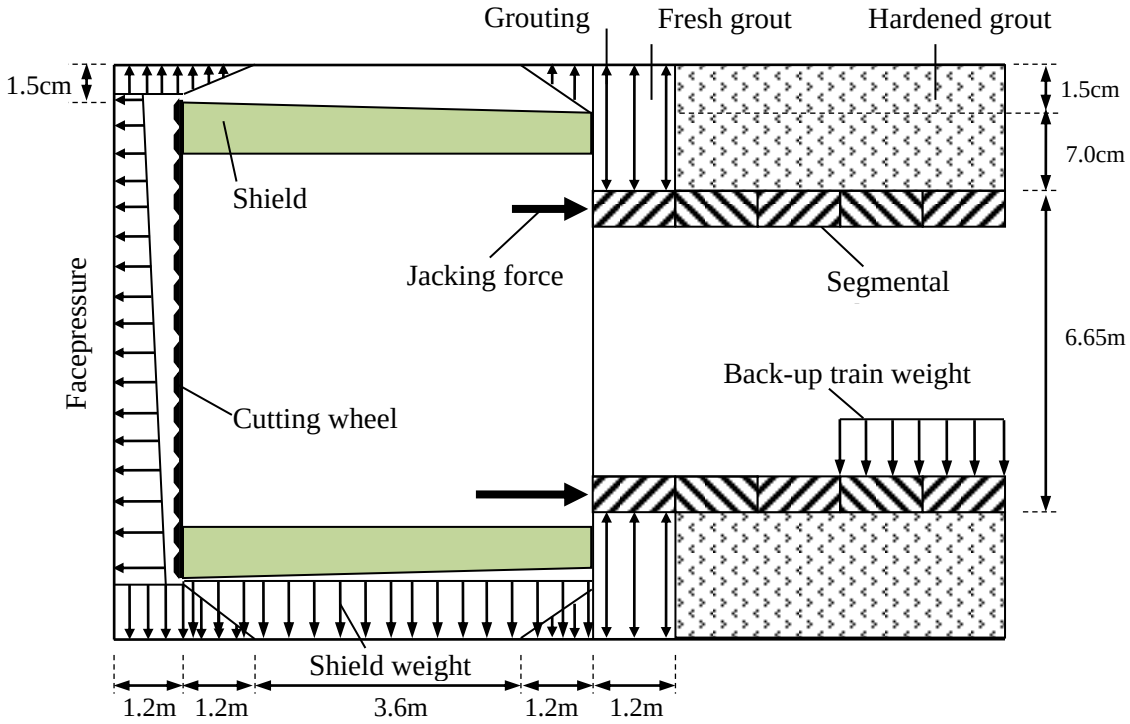

Figure 3. Layout of the proposed TBM model (not scaled)

The shield machine has been simulated using a "fictive" shield introduced by Mollon et al. (2013), Do et al. (2014a). Accordingly, the position of each point on the outside face of the shield was computed at each computation cycle of the numerical calculation process, and this position was artificially fixed when this point begins to be in contact with the "fictive" shield. The geometrical parameters of the shield are presented in Figure 3. The self-weight of the TBM-EPB is modeled through the vertical loads applied on the grid points of the ground mesh at the tunnel bottom area over an assumed range of 90 degrees in the cross-section and the whole shield length, as can be seen in Figs. 3, 4. In this study, the shield weight of 1650 kN is assumed to refer to an external diameter of 6.79 m and a length of 6 m measured from the tunnel face to the last installed lining ring at the shield tail.

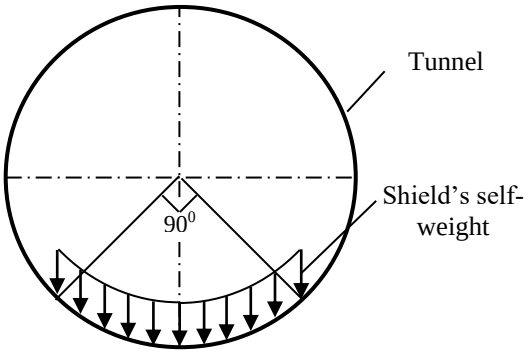

Figure 4. Self-weight scheme of the shield machine

The jacking force has been assumed to be linearly distributed over the height of the tunnel and set on each segment (Do et al., 2014a). Total jacking forces of 19,224 and 24,894 kN were adopted to apply in upper and lower tunnels, respectively.

The cement grout was injected at the shield tail section of both tunnels to fill the annular gap between the exterior surfaces of tunnel linings and the excavated ground surfaces. The grouting action is modeled in two phases: (1) the liquid phase represented by a certain pressure acting on the ground surface and the tunnel lining; (2) the hardened phase. The grouting pressures at the 160 and 400 kN tunnel crown were used in the upper and lower tunnels, respectively, based on the monitoring data obtained during the TBM-EPB operation. The grout was simulated as a uniform pressure and applied to both the excavated ground's cylindrical surface and the tunnel lining's exterior surface. Like the face pressure, a migration of fresh grout in the annular void between the outside surface of the shield and the excavated ground was assumed. This grouting migration was simulated employing a triangular pressure over the length of one ring (1.2 m). The real average advance rates of TBM-EPB of the lower and upper tunnels when passing the investigated section (0+980) are 4.8 and 2.99 meters per day. Assuming that it takes half a day for injected grout to reach its hardened phase (Shivaei et al., 2020), the grouting pressure was eliminated after installing two lining rings. Beyond this length, hardened grout was simulated through volume elements with elastic characteristics.

E_{grout}= 10 MPa and ν_{grout}= 0.22 (Do et al., 2014a).

The tunnel lining was modelled using a linear-elastic embedded liner element. Embedded liner elements are connected to the zone faces of the tunnel boundary. The linning-zone normal stiffness k_n and tangential stiffness k_s are chosen based on a recommended rule-of-thumb in which k_n and k_s are set to one hundred times the equivalent stiffness of the stiffest neighboring zone (Itasca, 2017). The stiffness of a zone in the perpendicular direction to the surface is defined as follows:

$$\max\left[\frac{\left(K+\frac{4}{3}G\right)}{\Delta z_{\min}}\right] \quad (1)$$

where: K and G = the bulk and shear modulus of soil, respectively;

z_{min} = the smallest dimension of an adjoining zone in the normal direction.

The segmental joints were simulated using double node connections. The stiffness characteristics of the segmental joint in a ring were represented by a set composed of a rotational spring (K_θ), an axial spring (K_A) and a radial spring (K_R). The joint between lining rings was also simulated using double connections with a set of rotational spring ($K_{\theta R}$), axial spring (K_{AR}) and radial spring (K_{RR}). The interaction mechanism of each spring is the same as that applied for a segment joint (Do et al., 2013).

To consider the TBM-EPB backup train during the excavation process in the numerical simulation, vertical downward distribution loads of a total weight of the backup train (1990 kN) were assigned on the lining elements at the tunnel bottom region over an assumed angle of 90 degrees in the cross-section and over a tunnel length of 72m behind the shield tail.

The studied structure is a simplification of the existing Haiyen building. While beam elements are used to model the beams and posts, shell elements modeled the floors and raft foundation. The thickness of the floors and raft is assumed to be 0.12 m and 0.3 m, respectively. Sides of squared columns and rectangular beams are, respectively, (0.3 × 0.3) m and (0.22 × 0.35) m. The

material properties are those of a long-term stick, and the behavior is elastic: Young's modulus E = 2.0 × 109 N/m^2 and Poisson's ratio ν = 0.2. The building is subject only to its own weight (unit weight of 25 kN/m^3). On a soil thickness of about 2.2 m under the model structure, the soil's behavior is elastic to avoid plastification of the soil areas during the placement of the structure.

Considering TBM working procedure, the twin stacked tunnel construction under the presence of the building is simulated in different steps in numerical models. In the first step, gravity stresses are applied, and the structure is introduced on the ground, then the numerical model is balanced. Once the equilibrium is reached, all the movements of the whole model are initialized to study only the influence of the tunnel excavation. The forces in the structure are not initiated, and an initial state of the structure in terms of internal forces is thus obtained. Afterward, the tunnel construction is modeled in several steps simulating the tunnel pass through the surface building.

The twin stacked tunnel excavation is modeled as follows: (i) excavation of the first lower tunnel (named tunnel T1); (ii) excavation of the second upper tunnel (named tunnel T2) after finishing the excavation of tunnel T1. The 3D model presented in Fig. 5 is 96 m in length in the Y direction, 160 m width in the X direction, and 54.07 m height in the Z direction. It consists of approximately 1,289,600 zones and 1,326,476 grid points. Regarding boundary conditions, while the model's bottom is fixed both in horizontal and vertical directions, vertical boundaries are fixed in the horizontal direction.

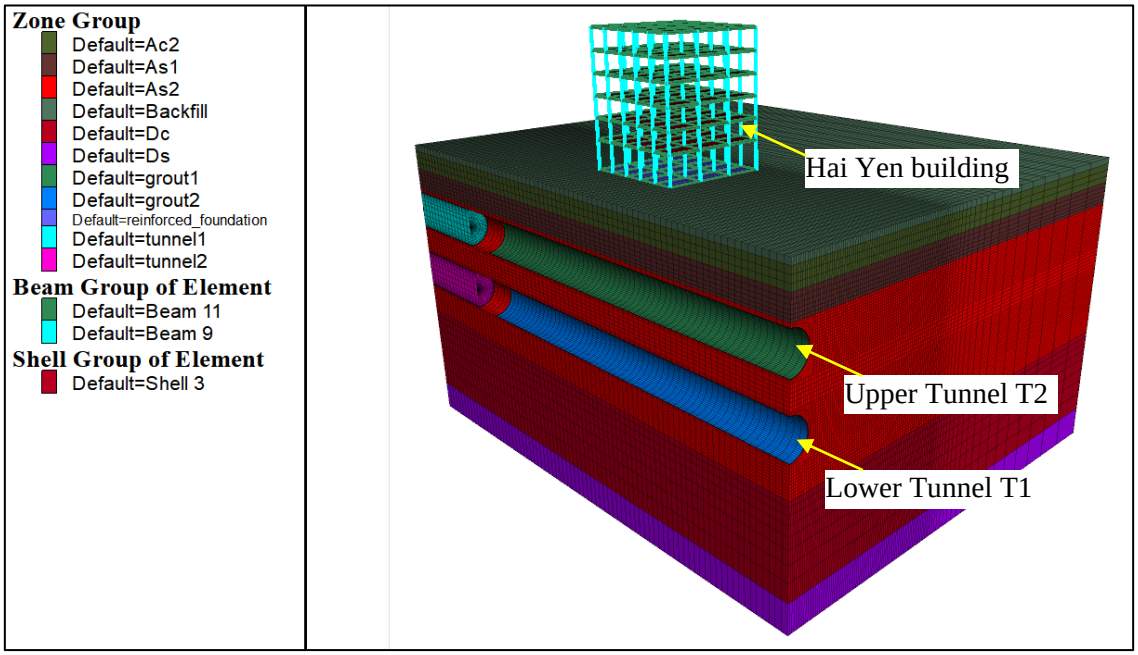

Figure 5. Cut of the 3D numerical model implemented

4. Verification of numerical model

Selection of the appropriate soil constitutive model is one of the greatest challenges faced by geotechnical engineers who do numerical simulations today. In this paper, the linear elastic-perfectly plastic

Mohr-Coulomb model (MC) and the Plasticity Hardening model (PH) have been adopted to evaluate the performance of these two soil constitutive models in estimating the surface settlement caused by twin stacked tunnel excavation. In contrast to the MC model, the PH model also accounts for stress-dependency of the stiffness modulus to increase when the stress increases. The plastic strains are calculated by introducing frictional yield hardening and cap hardening. The yield surface of a hardening plasticity model is therefore not fixed, but it can expand due to plastic straining. Properties of soil layers are presented in Table 3.

In Fig. 6, using input parameters at chainage 0+980 of Hochiminh's metro line 1 mentioned above, numerical normalized surface settlements caused by the excavation of twin stacked tunnels under a presence building are compared with the measurement data. It could be seen that the MC model estimates a narrower settlement trough and is much more different from measurement data. Meanwhile, the PH model predicts the settlement trough, which shows good compliance with measurement data. The constant stiffness of the MC model leads to inappropriate modeling of the settlement trough, whereas the behavior from the PH model agrees with the field observations. Based on that, the PH model is adopted for parametric study in the next section.

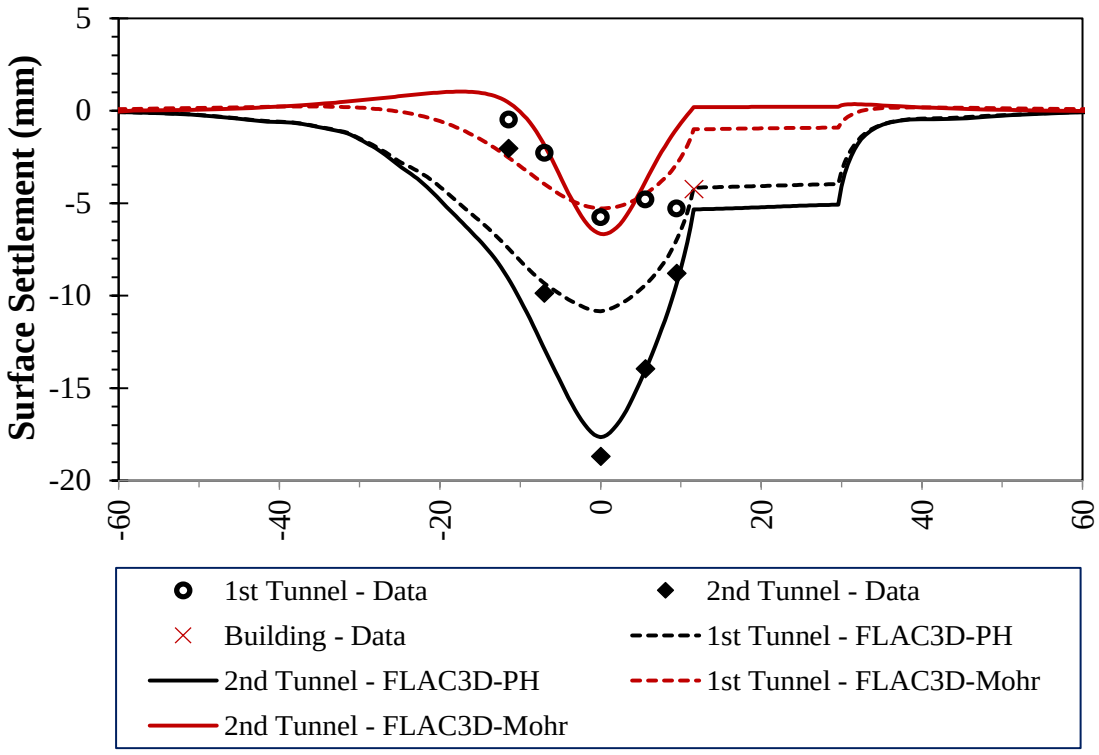

Figure 6. Comparison of settlement troughs over twin stacked tunnels

5. Parametric investigation of shield's operation parameters

In this section, the presence of building on the ground surface is not taken into account. The effect of the shield machine operation parameters on the surface settlements is investigated. Three main parameters are considered: face pressure, grouting pressure at

the shield tail, length and weight of the shield. For the comparison purpose, a reference case with the following parameters has been chosen:

- Face pressure (FP) equals the horizontal ground stress determined at the tunnels' center level. The face pressures of 180 kPa and 310 kPa at the upper and lower tunnels centers, respectively, were adopted.

- Grouting pressure at the shield tail (GP) equals a value of 1,2 times the vertical stress measured at the tunnels' crown. The grouting pressures of 160 kN and 400 kN were used in the upper and lower tunnels, respectively.

- Length of 6 m and weight of the shield of 1650 kN.

To highlight the effect of each parameter, the range used for the parametric study is presented in Table 4.

Table 4. Range of investigated operation parameters of the shield machine

N^0	Parameter	Unit	Range	Note
1	Face pressure	%	80; 90; 100; 120; 150; 175; 200	Percentage compared to the reference case
2	Shield tail grouting pressure	%	60; 80; 100; 120; 150; 200	Percentage compared to the reference case
3	Weight/Length of the shield	kN/m	1650/6; 1950/7.2; 2090/8.4; 2390/9.6	

5.1. Effect of the face pressure (FP)

Seven different values of the face pressure are used for the parametric analysis. The reference face pressure value (FP_{ref}) is assumed to be equal to the horizontal ground stress measured at the tunnel centre level and the corresponding maximum settlement value is hereafter called $S_{max\text{-}single\text{-}ref}$. Other values of the face pressure are respectively chosen as 80%, 90%, 120%, 150%, 175% and 200% of the reference value (FP_{ref}). The effect of face pressure on the maximum settlements (S_{max}) is presented in Fig. 7. It should be noted that when the face pressure is lower than 70%, the numerical model could not reach convergence. It means the instability of the tunnel face.

Figure 7 shows the same tendency of the maximum surface settlement (S_{max}) on the face pressure (FP) for the cases of a single lower tunnel and twin stacked tunnels. In the case of a single tunnel (i.e., lower tunnel T1), the maximum settlement S_{max} reaches a value of 113.5% and 104.4% of the $S_{max\text{-}single\text{-}ref}$ when the applied face pressure is equal to 80% and 90% of FP_{ref}, respectively. When the face pressure continuously increases (i.e., reach over values of 120%), the surface settlement tends to increase compared with that of reference face pressure value as seen in Fig. 7. While the larger settlement observed for a low face pressure (80% and 90% of FP_{ref}) is concerned by the immediate tunnel face movements (Kasper et al., 2006b; Chakeri et al., 2013), the settlements increase when the face pressure exceeds a value of 120% FP_{ref} can be explained by the division of the final settlement into 2 parts, i.e., immediate settlement in short term and the consolidation settlement induced in long term after the tunnel excavation (Kim et al., 2018).

Indeed, immediate settlements occur before and right after the tunnel face excavation. They are caused by the relaxation process induced in the soil mass by the tunnel excavation. Kim et al. (2018) indicated that the immediate settlements occurred ahead of the tunnel face. They decrease when the tunnel face pressure increase. However, concerning the immediate settlements induced at the back of the tunnel face and just after the passage of the cutter head, when the face pressure increases from low values to a higher percentage of the reference face pressure value, the immediate settlements gradually decrease their minimum value. Beyond this minimum value, the immediate settlements on

the back of the tunnel face begin to increase with the face pressure increase (Kim et al., 2018).

The consolidation settlements depend on the effective stress variations induced at the tunnel vicinity (Kim et al., 2018). A critical face pressure value that leads to the value of a minimum settlement is observed. Firstly, the consolidation settlements decrease with the face pressure increase, and then their values increase when the face pressure overpass the critical value.

At the final or steady-state, the surface settlements induced by the tunnel excavation in this study combine immediate and consolidation settlements. They have the same variation tendency and depend on the face pressure. The same results were obtained for the case of a single tunnel by Kim et al. (2018). In other words, a critical value of the face pressure of more or less 100% FP_{ref} is recommended in this study in terms of minimum surface settlements (Fig. 7).

For the case of twin stacked tunnels, the excavation of the second upper tunnel (T2) causes a settlement increase, as seen in Fig. 7. The same settlement variation tendency with the face pressure as for the single tunnel case is observed. The critical face pressure value at which the minimum settlement induced over the twin stacked tunnels is reached is also close to 100% FP_{ref} (Fig. 7).

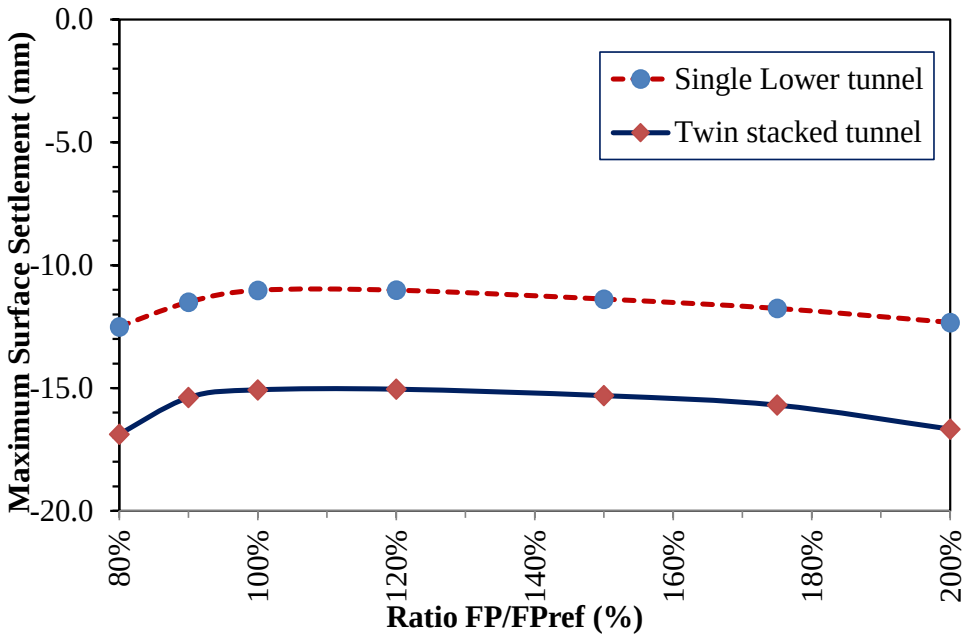

Figure 7. Relationship between the maximum surface settlement with the tunnel face pressure

5.2. Effect of the grouting pressure at the shield tail (GP)

Grouting pressures are assumed to be linearly distributed and increased from the top to the tunnel bottom to take into consideration the influence of the fresh grout density (20 kN/m^3). The reference grouting pressure (GP_{ref}) is taken equal to 1.2 times the vertical ground pressure at the tunnel top. Different GP values of 60%, 80%, 120%, 150% and 200% of the reference value (GP_{ref}) are considered in this study.

In Fig. 8, the settlements with the grouting pressure variation are illustrated. The grouting pressure acts for a short period on the ground surrounding the shield tail, and then it will be hardened. Therefore, the grouting pressure

impacts only the immediate settlements at the shield tail. Immediate settlements gradually decrease with the grouting pressure increase (Kim et al., 2018). However, as the consolidation settlements depend strongly on the effective stresses (Kim et al., 2018), when the grouting pressure increase and reaches the GPref value, the settlements induced by the excavation of the first tunnel are insignificantly changed. Beyond the value of reference grouting pressure (GPref), settlements begin to lightly increase with a rising grouting pressure, as seen in Fig. 8. The maximum settlement developed for twin stacked tunnels at the steady-state shows the same dependency with the grouting pressure (Fig. 8). Therefore, a maximum value of the grouting pressure equal to GPref is recommended in this study to limit the settlements induced by a single lower tunnel and twin stacked tunnels.

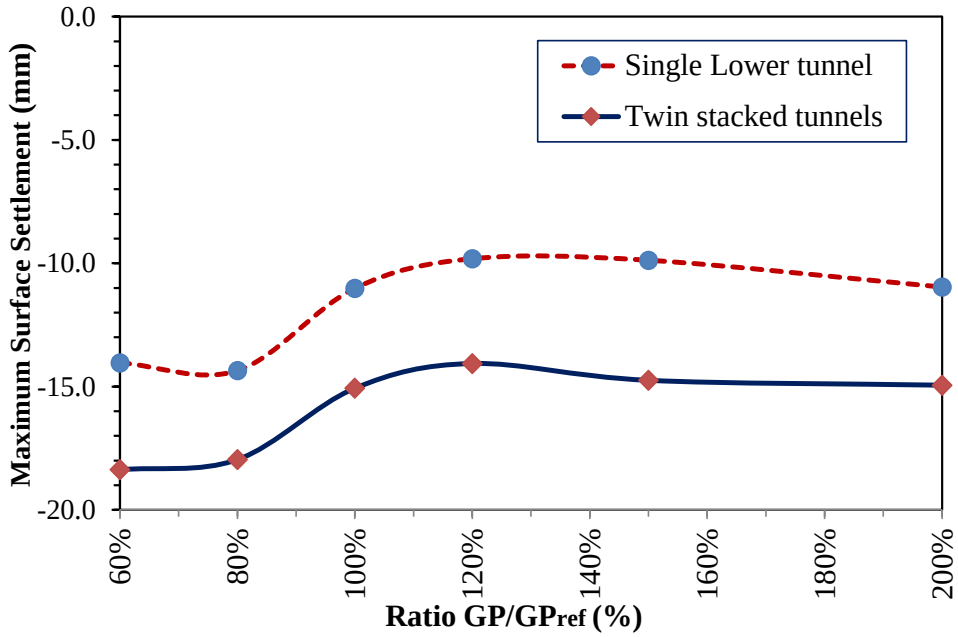

Figure 8. Dependence of maximum surface settlement on the grouting pressure applied at the shield tail

5.3. Effect of the shield length

This section describes the effect of shield length on the surface settlement developed over twin stacked tunnels. It should be mentioned that a longer shield corresponds to a heavier shield. Parameters of the shield length and corresponding weights are shown in Table 3.

When using a short shield length of 6.0m, the settlement developed at the ground surface is smaller than in cases where longer shields are used (7.2 m, 8.4 m, and 9.6 m) (Fig. 9). Under the impact of vertical loads caused by the shield weight distributed over the bottom and along the length of the shied machine, downward movement of the tunnel is predicted. The longer the zone is loaded by the heavier shield machine, the greater the downward movement and, therefore, the surface settlements. Another reason could be concerned with the fact that the shorter shield length is not long enough to allow immediate settlements to be fully developed before the tunnel lining installation. It is reasonable to conclude that a shield length of 6 m should be recommended to use. Figure 9 also indicates that settlements increase after the second upper tunnel excavation.

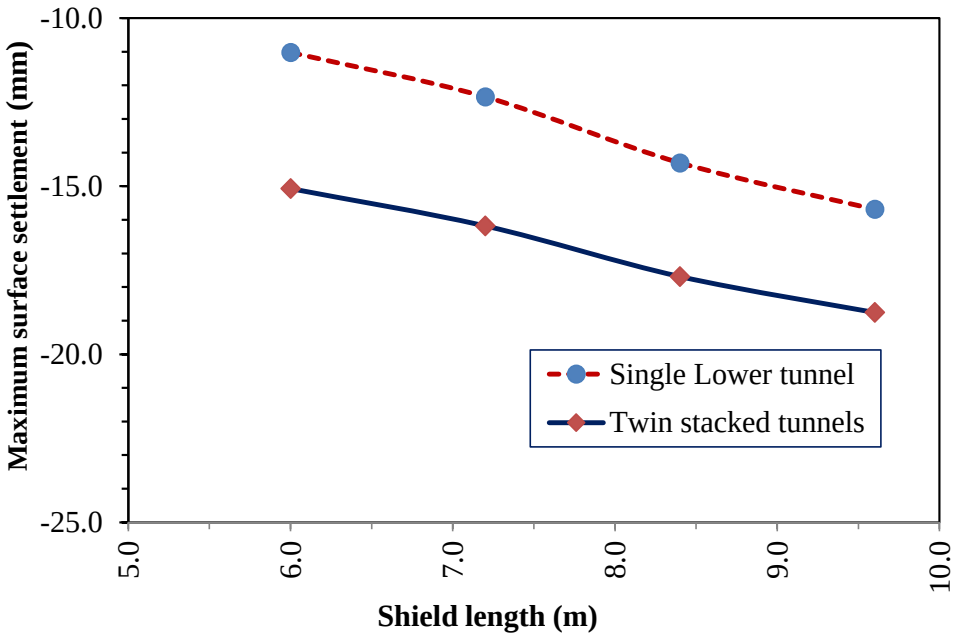

Figure 9. Dependence of maximum surface settlement on the shield length

6. Conclusions

The influence of the face support pressure, grouting pressure, and shield length on the surface settlements developed over twin stacked tunnels excavated by shield machines are analyzed utilizing three-dimensional numerical models. The analyses indicate the importance of using appropriate operating parameters of the shield machine during the tunnel excavation. The findings of this study are:

- The Mohr-Coulomb constitutive model is not appropriate to estimate the settlement induced by tunnel excavation. An advanced constitutive model allowing considering the change of stiffness modulus, such as Plasticity Hardening, should be used.

- The surface settlement developed over tunnels at the steady-state should be predicted considering both immediate settlement in a short time and consolidation settlement in a long time;

- A critical value of the face pressure of 100% FPref is recommended in this study for minimum surface settlements over the single lower tunnel and twin stacked tunnels. An increase in the face pressure is not always followed by a decrease in surface settlements.

- A minimum value of the grouting pressure equal to GPref is recommended in this study to limit the settlements induced by a single lower tunnel and twin stacked tunnels.

- Shorter shield machines cause smaller surface settlements to develop over single lower and twin stacked tunnels.

- Twin stacked tunnels excavation causes an increase of the settlements compared to that of a single lower tunnel excavated first.

Acknowledgments

This research is funded by the Vietnam National Foundation for Science and Technology Development (NAFOSTED) under grant number 105.08-2018.310.

References

Chakeri H., Ozcelik Y., Unver B., 2013. Effects of important factors on surface settlement prediction for metro tunnel excavated by EPB. Tunnelling and Underground Space Technology, 36, 14-23.

Chakeri H., Ozcelik Y., Unver B., 2014. Investigation of ground surface settlement in twin tunnels driven with EPBM in urban area. Arab. J. Geosci. Doi: 10.1007/s12517-014-1722-2.

Chapman D.N., Ahn S.K., Hunt D.V., 2007. Investigating ground movements caused by the construction of multiple tunnels in soft ground using laboratory model tests. Canadian Geotechnical Journal, 44(6), 631-643.

Chen R.P., Zhu J., Liu W., Tang X.W., 2011. Ground movement induced by parallel EPB tunnels in silty soils. Tunnelling and Underground Space Technology, 26, 163-171.

Do N.A., Dias D., Oreste P.P., Djeran-Maigre I., 2013. Three-dimensional numerical simulation for mechanized tunnelling in soft ground: The influence of the joint pattern. Acta Geotechnica, 9(4), 673-694.

Do N.A., Dias D., Oreste P.P., Djeran-Maigre I., 2014a. Three-dimensional Numerical Simulation of a Mechanized Twin Tunnels in Soft Ground. Tunnelling and Underground Space Technology, 42, 40-51.

Do N.A., Dias D., Oreste P.P., 2014b. Three-dimensional numerical simulation of mechanized twin stacked tunnels in soft ground. Journal of Zhejiang University Science A, 15(11), 896-913.

Ercelebi S.G., Copour H., Ocak I., 2011. Surface settlement predictions for Istanbul metro tunnels excavated by EPB-TBM. Springer. Environ. Earth Sci., 62, 357-365.

Hanoi Metropolitan Railway Management Board (MRB). Hanoi Pilot Light Metro Line 3, Section Nhon-Hanoi Railway Station-Technical Design of Underground Section-Line and Stations, Package number: HPLMLP/CP-03.2012.

Hasanpour R., Chakeri H., Ozcelik Y., Denek H., 2012. Evaluation of surface settlements in the Istanbul metro in terms of analytical, numerical and direct measurements. Bull. Eng. Geol. Environ., 71, 499-510.

Ho Chi Minh City Urban Railway Construction Project (HUP), Ben Thanh - Suoi Tien Section (Line 1). Contract Package-1b: Civil (Underground Section KM 0+615 to KM 2+360): Bored tunnel - Segmental lining - Technical design report, 2016.

Itasca Consulting Group. FLAC fast Lagrangian analysis of continua, version 6.0. User's manual, 2017.

Janin J.P., Dias D., Emeriault F., Kastner R., Bissonnais H., Guilloux A., 2015. Numerical back-analysis of the southern Toulon tunnel measurements: a comparison of 3D and 2D approaches, Engineering Geology, 195, 42-52.

Kasper T., Meschke G., 2006a. A numerical study of the effect of soil and grout material properties and cover depth in shield tunnelling. Comput Geotech, 33(4-5), 234-247.

Kasper T., Meschke G., 2006b. On the influence of face pressure, grouting pressure and TBM design in soft ground tunnelling. Tunnelling and Underground Space Technology, 21, 160-171.

Kim K., Oh J., Lee H., Kim D., Choi H., 2018. Critical face pressure and backfill pressure in shield TBM tunneling on soft ground. Geomechanics and Engineering, 15(3), 823-831.

Kim S.H., Burd H.J., Milligan G.W., 1998. Model testing of closely spaced tunnels in clay. Geotechnique, 48(3), 375-388.

Kuriki M., 2020. Design and construction of first bored tunnel under Ho Chi Minh City Metro Line 1 in Vietnam. International Conference GEOTEC HANOI 2019, Geotechnics for Sustainable Infrastructure Development, Lecture Notes in Civil Engineering ISBN 978-981-15-2183-6, pp 221-228. Doi.org/10.1007/978-981-15-2184-3

Lu H., Shi J., Wang Y., Wang R., 2019. Centrifuge modeling of tunneling-induced ground surface settlement in sand. Underground Space, 4(4). Doi.org/10.1016/j.undsp.2019.03.007.

Ly H.B., Nguyen H.L., Do M.N., 2021. Finite element modeling of fluid flow in fractured porous media using unified approach. Vietnam Journal of Earth Sciences, 43 (1), 13-22.

Melis M., Medina L., Rodriguez J., 2002. Prediction and analysis of subsidence induced by shield tunnelling in the Madrid Metro extension. Can. Geotech. J., 39, 1273-1287.

Mirhabibi A., Soroush A., 2013. Effects of building three-dimensional modeling type on twin tunneling-induced ground settlement. Tunnelling and Underground Space Technology, 38, 224-234.

Ng C.W., Lu H., Peng S.Y., 2013. Three-dimensional centrifuge modelling of the efects of twin tunnelling on an existing pile. Tunnelling and Underground Space, 35, 189-199.

Nguyen T.H., Pham H.G., Phien-wej., 2020. Tunneling induced ground settlements in the first metro line of Ho Chi Minh City, Vietnam. International Conference GEOTEC HANOI 2019, Geotechnics for Sustainable Infrastructure Development, Lecture Notes in Civil Engineering ISBN 978-981-15-2183-6, pp 297-304. Doi.org/10.1007/978-981-15-2184-3

Ocak I., 2013. Interaction of longitudinal surface settlements for twin tunnels in shallow and soft soils: the case of Istanbul Metro. Environ. Earth Sci., 69, 1673-1683.

Sahoo J.P., Kumar J., 2018. Required Lining Pressure for the Stability of Twin Circular Tunnels in Soils. International Journal of Geomechanics, 18(7), 04018069.
Doi: 10.1061/(asce)gm.1943-5622.0001196.

Shivaei S., Hataf N., Pirastehfar K., 2020. 3D numerical investigation of the coupled interaction behavior between mechanized twin tunnels and groundwater - A case study: Shiraz metro line. Tunnelling and Underground Space Technology, 103. Doi.org/10.1016/j.tust.2020.103458.

Suwansawat S., Einstein H.H., 2007. Describing settlement troughs over twin tunnels using a superposition technique. Journal of Geotechnical and Geoenvironmental Engineering, 133(4), 445-468.

Tran T.N., Hiroshi M., 2020. Pore water pressure accumulation and settlement of clays with a wide range of Atterberg's limits subjected to multi-directional cyclic shear. Vietnam Journal of Earth Sciences, 42 (1), 93-104.

Wang H.N., Wu L., Jiang M.J., Song F., 2018. Analytical stress and displacement due to twin tunneling in an elastic semi-infinite ground subjected to surcharge loads. International Journal for Numerical and Analytical Methods in Geomechanics, 42(6), 809-828. Doi:10.1002/nag.2764.

Wang J.G., Kong S.L., Leung C.F., 2003. Twin tunnels-induced ground settlement in soft soil. Proceeding of the Sino-Japanese Symposium on Geotechnical Engineering, Beijing, China, 241-244.

Yang X.L., Wang J.M., 2011. Ground movement prediction for tunnels using simplified procedure. Tunnelling and Underground Space Technology, 26, 462-471.

Zhang Z., et al., 2018. Complex variable solutions for soil and liner deformation due to tunneling in clays. International Journal of Geomechanics, 18(7), Doi.org/10.1061/(ASCE)GM.1943-5622.0001197.

Zhang Z., Huang M., Zhang C., Jiang K., 2020. Complex Variable Solution for Twin Tunneling-Induced Ground Movements Considering Nonuniform Convergence Pattern. International Journal of Geomechanics, 20(6). Doi.org/10.1061/(ASCE)GM.1943-5622.0001700.

Zhao C., Schmüdderich C., Barciaga T., Röchter L., 2019. Response of building to shallow tunnel excavation in different types of soil. Computers and Geotechnics, 115. Doi.org/10.1016/j.compgeo.2019.103165.